

Late Holocene fluctuations of the north lobe of Llewellyn Glacier, Upper Yukon River Basin

M. Samolczyk¹

School of Science, Yukon College

S. Laxton

Yukon Geological Survey

J.J. Clague

Department of Earth Sciences, Simon Fraser University

Samolczyk, M., Laxton, S. and Clague, J.J., 2016. Late Holocene fluctuations of the north lobe of Llewellyn Glacier, Upper Yukon River Basin. *In: Yukon Exploration and Geology 2015*, K.E. MacFarlane and M.G. Nordling (eds.), Yukon Geological Survey, p. 223-231.

ABSTRACT

Llewellyn Glacier contributes glacial meltwater to runoff entering the Yukon River, which flows through the hydroelectric power dam in Whitehorse, Yukon. An examination of lateral moraine stratigraphy, and radiocarbon and dendrochronological dating of *in situ* and detrital subfossil wood provide a record of fluctuations of Llewellyn Glacier over the past two millennia. Our data indicate the north lobe advanced sometime between AD 260 and AD 505, and reached within 70 m of its Little Ice Age maximum limit as early as the 17th century. The main lobe advanced as early as AD 1035, possibly between the First Millennium and Little Ice Age advances of the last two millennia, when glaciers have traditionally been considered more restricted. Results provide new information on the timing and frequency of fluctuations of Llewellyn Glacier, and can be used to assist with modelling the future impacts of climate change on glacial meltwater contributions to rivers and hydroelectric security in Yukon.

¹msamolczyk@yukoncollege.yk.ca

INTRODUCTION

Glaciers at the headwaters of the Yukon River are important sources of the water that flows through the hydroelectric power dam in Whitehorse, Yukon. Concern over the impacts of climate change on hydroelectric security in Yukon has prompted examination of the contribution of glacial meltwater to runoff in the Upper Yukon River Basin, the fourth largest drainage basin in North America (Brabets *et al.*, 2000; Northern Climate Exchange, 2014). Llewellyn Glacier, an eastward flowing outlet glacier of the Juneau Icefield in British Columbia, contains at least half of the total ice in the Upper Yukon River Basin and was the single greatest contributor to runoff from glacier melt (7.3%) and glacier wastage (2.7%), as defined by Comeau *et al.* (2009), between 1981 and 2011 (Northern Climate Exchange, 2014).

Most glaciers around the world have thinned and retreated; cumulative losses of ice have increased from 226 Gt/year between 1971 and 2009 to 301 Gt/year between 2005 and 2009 (IPCC, 2013). In Yukon, the total area of glacier ice cover has decreased by 22% since the 1957-1958 International Geophysical Year (Barrand and Sharp, 2010). Like most other glaciers in Yukon, Llewellyn Glacier has thinned and retreated rapidly over the past several decades (Sprenke *et al.*, 1999; Clague *et al.*, 2010). Based on an analysis of remotely sensed and GIS data, the surface area of Llewellyn Glacier decreased 8.3% from 1948 to 2010 (Northern Climate Exchange, 2014).

Glaciers are sensitive to even minor changes in climate, and studies of geologic and dendrochronologic records in glacier forefields may provide evidence of past climatic conditions (Denton and Karlén, 1973). This paper presents evidence of recent fluctuations of the north lobe of Llewellyn Glacier. Our objective is to document the response of Llewellyn Glacier to past environmental change, which may provide insight into how the glacier will respond to future climate warming.

PREVIOUS WORK

Investigations based on Shuttle Radar Topographic Mission digital elevation model (SRTM DEM) data and Canadian digital elevation data (CDED DEM) indicate that the elevation of the surface of the lower part of Llewellyn Glacier decreased nearly 100 m between 1987 and 2000 (Northern Climate Exchange, 2014). Clague *et al.* (2010) studied the forefield of the main and south lobes of Llewellyn Glacier to construct a record of

glacier expansion during the past two millennia. Based on the stratigraphy of lacustrine and deltaic sediments and on tree-ring and radiocarbon ages of detrital wood and glacially overridden stumps in growth position, they concluded that the glacier advanced between AD 300 and AD 500 and between AD 1035 and AD 1210, reaching within 400 m of its Little Ice Age (LIA) maximum limit in the later advance. The times of these advances are not fully consistent with previous interpretations that glaciers in northwest North America advanced during two broad intervals in the past two millennia: one near the start of the first millennium AD, referred to as the First Millennium Advance (FMA; Reyes *et al.*, 2006); and a second during the Little Ice Age (LIA), which began around AD 1200 and culminated in the eighteenth and nineteenth centuries (Clague *et al.*, 2010). Clague *et al.* (2010) argued that glacier behavior in northwest North America during the past two millennia is more complex than this simple view would suggest. Investigations at Bromley Glacier (Hoffman and Smith, 2013) and at Franklin Glacier (Mood and Smith, 2015) support this interpretation by showing that these glaciers advanced during the period between the FMA and LIA. Our study provides additional data pertinent to this issue from the north lobe of Llewellyn Glacier, which has not been previously examined.

STUDY AREA

Llewellyn Glacier, with an area of approximately 427 km², is one of the largest glaciers in British Columbia (Arendt *et al.*, 2014). It flows east from the Juneau Icefield toward the southern end of Atlin Lake (Fig. 1). The Juneau Icefield lies at the crest of the northern Boundary Ranges of the Coast Mountains and is the fifth largest icefield (4000 km²) in North America (Sprenke *et al.*, 1999). Llewellyn Glacier flows from elevations of 1830 to 1980 m above sea level and terminates in three lobes between about 700 and 900 m above sea level. The largest lobe (herein referred to as the 'main' lobe) flows east and two smaller lobes, the 'north' and 'south' lobes, are located, respectively, north and south of the main lobe. Extensive lateral and end moraines, as well as trimlines, are preserved in the forefield area of the glacier and mark its maximum Holocene extent.

A weather station in Atlin BC, 54 km northeast of the toe of the north lobe of Llewellyn Glacier, records daily average January and July temperatures of -12.8°C and 13.4°C, respectively (Environment Canada, 2015). Average precipitation for January and July is 45.6 mm and 32.8 mm (water equivalent), respectively.

Our focus was on the lateral and end moraines of the north lobe of Llewellyn Glacier (study area 1; Fig. 1). An additional site on the north lateral moraine of the main lobe, approximately 4 km from its terminus, was also examined (study area 2; Fig. 1). Meltwater issuing from the north lobe enters a small proglacial lake and then flows into Hobo Creek, which discharges into Willison Bay of Atlin Lake. The north lobe occupies a narrow valley (~1.5 km wide) flanked by lateral moraines and is approximately 3.5 km long, terminating about 2.6 km up-valley from a sharp-crested LIA end moraine.

METHODS

The stratigraphy of lateral moraines was examined and recorded in June and August 2014 and samples of *in situ* and detrital subfossil wood associated with paleosurfaces of older buried moraines were collected for

radiocarbon dating. Additional samples were collected for dendrochronologic analysis from living and dead trees on the distal slope of an end moraine of the north lobe (Fig. 1). Radiocarbon ages of the outer rings of glacially overridden, *in situ* stumps date the time when a glacier advanced over and killed the trees. *In situ* wood also provides a minimum age for the surface on which it grew. Ages of detrital wood are more difficult to interpret, but nevertheless, in the case of till, detrital wood ages are maxima for the time of deposition from ice with enclosing sediments at the location from which the wood was recovered.

Eleven samples of wood were radiocarbon dated using the accelerator mass spectrometry (AMS) method at Beta Analytic Inc. and the Keck Carbon Cycle AMS facilities (Table 1). Radiocarbon ages were calibrated using the calibration dataset of Reimer *et al.* (2013) in OxCal v. 4.2.4 (Bronk Ramsey, 2013). Calibrated ages in brackets are

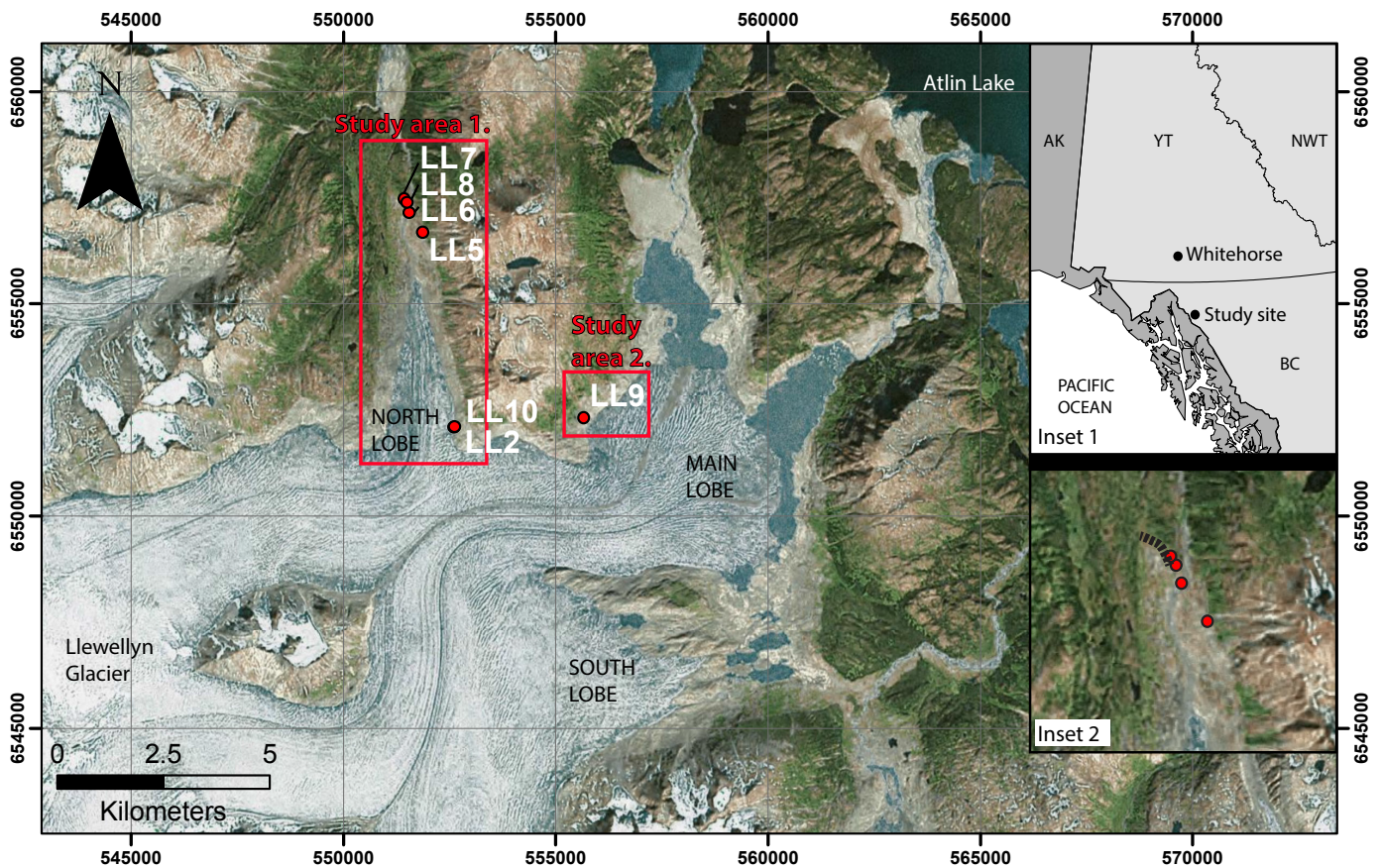


Figure 1. Satellite imagery of Llewellyn Glacier, British Columbia, Canada, with study areas 1 and 2 outlined (numbered black boxes). Red dots indicate location of sample sites. Inset map 1 shows location of Llewellyn Glacier relative to Whitehorse, Yukon. Inset map 2 shows close-up of sites LL5 to LL8 in study area 1 with dashed black line showing crest of the end moraine. Background imagery: Esri, DigitalGlobe, GeoEye, Earthstar Geographics, CNES/Airbus DS, USDA, USGS, AEX, Getmapping, Aerogrid, IGN, IGP, swisstopo and the GIS.

Table 1. Sample site locations and reported radiocarbon ages.

Radiocarbon age (¹⁴ C yr BP) ^a	Calendric age (AD) ^b	Laboratory number ^c	Site number (Fig. 1)	UTM coordinate (zone 8N)	Elevation (m)	Dated material
1705±30	252 - 401	UCIAMS-149293	LL2	552612, 6552090	1099	Branch or root ^d
1750±30	222 - 385	Beta-384639	LL2	552612, 6552090	1099	Branch or root ^e
1665±30	258 - 506	UCIAMS-149294	LL2	552612, 6552090	1099	Woody organic fragments
185±30	1650 - present	UCIAMS-149295	LL5	551867, 6556683	949	Branch or root ^e
80±30	1690 - 1926	UCIAMS-149296	LL6	551555, 6557143	797	Tree stump ^{e,f}
370±30	1446 - 1634	UCIAMS-149297	LL6	551555, 6557143	797	Tree stump ^{d,f}
145±30	1668 - 1948	UCIAMS-149298	LL7c	551427, 6557486	874	Tree trunk ^{d,g}
155±30	1666 - present	UCIAMS-149300	LL8	551503, 6557383	875	Branch or root ^e
910±30	1033 - 1204	UCIAMS-149301	LL9	555636, 6552368	834	Branch or root ^e
1775±30	138 - 339	UCIAMS-149302	LL10	552622, 6552092	unknown	Tree trunk ^d
1785±30	134 - 332	UCIAMS-149303	LL10	552622, 6552092	unknown	Tree trunk ^e

^aError terms reported by Laboratories are 1 σ

^bAge determined from the calibration curve of Reimer *et al.* (2013) in OxCal v.4.2.4 (2 σ ranges reported).

^cLaboratories: UCIAMS, Keck Carbon Cycle AMS Facility; Beta, Beta Analytic Inc.

^dInner wood

^eOuter wood

^fSample contains 136 rings

^gSample contains 147 rings

reported as 2 σ ranges and rounded to the nearest decade or mid-decade year. Three samples of wood were dated using dendrochronology. Disks from the trees were cut with a chainsaw, air-dried, and sanded with progressively finer sand paper until the ring boundaries were clearly discernable. Tree rings were counted at the University of Victoria Tree-Ring Laboratory using a WinDENDRO™ tree-ring imaging system (Guay *et al.*, 1992).

RESULTS

STUDY AREA 1 – NORTH LOBE OF LLEWELLYN GLACIER

Paleosurfaces containing subfossil tree fragments were found at three sites along the east lateral moraine of the north lobe of Llewellyn Glacier (LL2, LL10 and LL5) and at two sites on the valley floor within 100 m of the LIA end moraine (LL6 and LL8; Fig. 1). Tilted dead and living trees growing just behind the LIA end moraine were also dated (LL7; Fig. 1).

A well-developed buried paleosol containing woody debris and two organic horizons is exposed at site LL2 on the flank of the east lateral moraine, approximately 77 m above the glacier surface and about 500 m down-valley from where the north lobe separates from the main lobe

(Fig. 2a,b). A 1 m vertical section through the paleosol is exposed on the fresh steep face of the lateral moraine. The upper organic horizon, <35 cm thick, contains woody fragments, plant macrofossils and roots up to 15 cm in diameter in an olive-gray to brown mottled silt. This unit grades downward into a 52-cm-thick, yellow-brown sandy silt to silty sand containing discontinuous black peat lenses. A sharp contact separates the sand-silt unit from a lower, 1–2-cm-thick, organic horizon that contains black peat with woody roots and rootlets. An oxidized gravel unit, approximately 10-cm-thick, underlies the lower organic horizon and grades into till at the base of the section. A sample of the outer rings of a 15 cm-diameter branch or root from the upper organic horizon and another sample of its pith and adjacent inner rings, yielded radiocarbon ages, respectively, of 1750±30 ¹⁴C yr BP (AD 220-385; Beta-384639) and 1705±30 ¹⁴C yr BP (AD 250-400; UCIAMS 149293). A sample of the peat from the lower organic horizon returned a radiocarbon age of 1665±30 ¹⁴C yr BP (AD 260-505; UCIAMS-149294).

An *in situ* subfossil tree stump is exposed at site LL10 (Fig. 3), approximately 15 m down-valley from site LL2 and at about the same height (76 m) above the glacier surface. At this site, the steeply sloping bedrock surface crops out on the face of the east lateral moraine and the stump is rooted at the till-bedrock contact on the stoss side of the

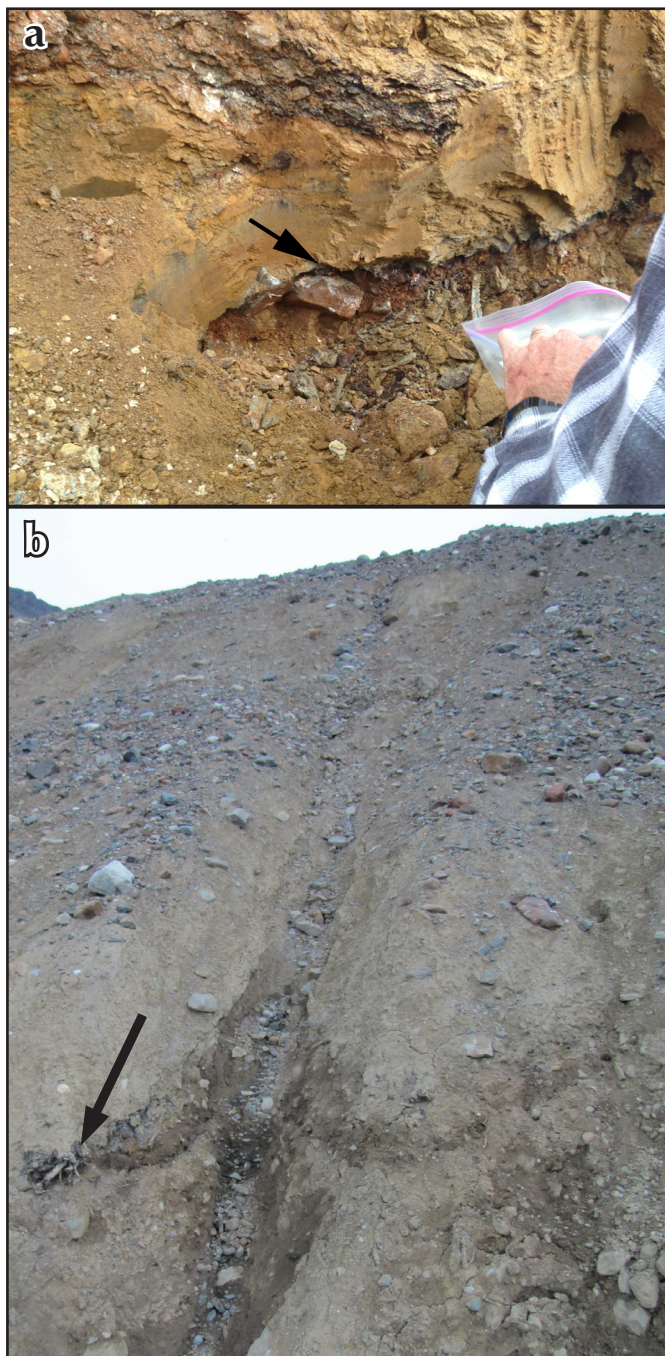


Figure 2. (a) Excavation at site LL2 showing the dated lower organic horizon (1–2 cm thick; indicated by an arrow). Also shown are the overlying yellow-brown sand-silt unit (~50 cm thick) and the underlying oxidized yellow-brown gravel. The dated upper organic horizon that overlies the sand-silt unit is not shown in this image. Person for scale. (b) Location of site LL2 below the right lateral moraine crest of the north lobe of Llewellyn Glacier. Arrow indicates location of wood protruding from the dated upper organic horizon. The paleosol is located approximately 30 m below the moraine crest.



Figure 3. Sheared tree stump shown protruding from contact between till and bedrock outcrop at site LL10. Northward ice flow direction is indicated by arrow. Photographer is aiming camera down the face of the east lateral moraine toward the base of the moraine. Pencil for scale.

bedrock exposure. Samples of the outermost rings and the pith and adjacent rings of the stump yielded radiocarbon ages of, respectively, 1785 ± 30 ^{14}C yr BP (AD 135-330; UCIAMS-149303) and 1775 ± 30 ^{14}C yr BP (AD 135-340; UCIAMS-149302).

At site LL5, 5.3 km down-valley from where the north lobe separates from the main lobe and 1.8 km beyond the terminus of the glacier, a paleosol containing a dark brown organic horizon with fibrous peat and *in situ* roots and fragments of detrital wood dips 30° from near the crest of the east lateral moraine toward the valley floor (Fig. 4). Fifteen to 30 cm of altered sediments with orange staining directly underlie the organic horizon, which can be traced discontinuously along the proximal slope of the moraine in gully exposures for about 20 to 30 m until it is about 15 m below the moraine crest. A gray matrix-



Figure 4. Dipping paleosol at site LL5, showing exposed organic horizon. Moraine crest lies approximately 0.5 m above the paleosol. Pencil for scale.

supported diamicton composed of a silt-sand matrix and 25–30% subangular to rounded clasts (cobble- to boulder-size), some with striations, overlies the organic horizon. A grayish-brown clast- to matrix-supported diamicton with angular to sub-angular clasts, as large as boulder-sized, underlies the organic horizon. The entire package is weakly stratified and dips 30° towards the valley floor. The outer rings of a 10 cm diameter, *in situ* tree stem protruding from the organic horizon near the moraine crest yielded a radiocarbon age of 185 ± 30 ^{14}C yr BP (AD 1650-present; UCIAMS-149295). The same horizon approximately 25 m farther down-valley comprises a large wood mat with several protruding stems, but was inaccessible.

An *in situ* subfossil tree stump about 30 cm in diameter with 136 rings was found in the forefield area of the north lobe, just up-valley (<70 m) from the LIA end moraine at site LL6 (Fig. 5). In this area, ice flowed over and around both sides of a large bedrock knob on the valley floor. Hobo Creek has incised through till on the east side of the bedrock knob, leaving a thin discontinuous veneer of till or reworked diamicton on the flank of the knob. The roots of the glacially sheared stump penetrate a bedrock crevice about 6.8 m above Hobo Creek. A sample of the outermost rings and another comprising the pith and adjacent rings yielded radiocarbon ages of, respectively, 80 ± 30 ^{14}C yr BP (AD 1690-1925; UCIAMS-149296) and 370 ± 30 ^{14}C yr BP (AD 1445-1635; UCIAMS-149297).



Figure 5. Sample LL6, an *in situ* tree stump sheared by a glacial advance. Handheld radio for scale.

The sharp-crested end moraine of the north lobe of Llewellyn Glacier abuts the aforementioned bedrock knob on its west side. The top of the bedrock knob is vegetated with a mature stand of subalpine fir (*Abies lasiocarpa* (Hooker) Nuttall), slide alder (*Alnus viridis* (Chaix) DC.) and shrubs. Tilted dead and live subalpine fir trees are present on the distal side of the moraine crest. At site LL7, a tilted, living subalpine fir with 147 rings growing on the distal side of the moraine, 4 m below its crest, had cambial scars on the proximal side of the trunk (sample LL7c; Fig. 6a,b). The inner pith and adjacent rings of this tree returned a radiocarbon age of 145 ± 30 ^{14}C yr BP (AD 1670-1950; UCIAMS-149298). Another living subalpine fir (sample LL7b), which had been damaged and was leaning along the ground, had 95 growth rings, but was not radiocarbon dated.

A patchy veneer of till with weakly developed O and A soil horizons overlies bedrock at the top of the bedrock knob at site LL8, only metres down-valley from site LL6 (Fig. 7). Outer rings of a detrital branch 20 cm below the soil surface returned a radiocarbon age of 155 ± 30 ^{14}C yr BP (AD 1665-present; UCIAMS-149300).

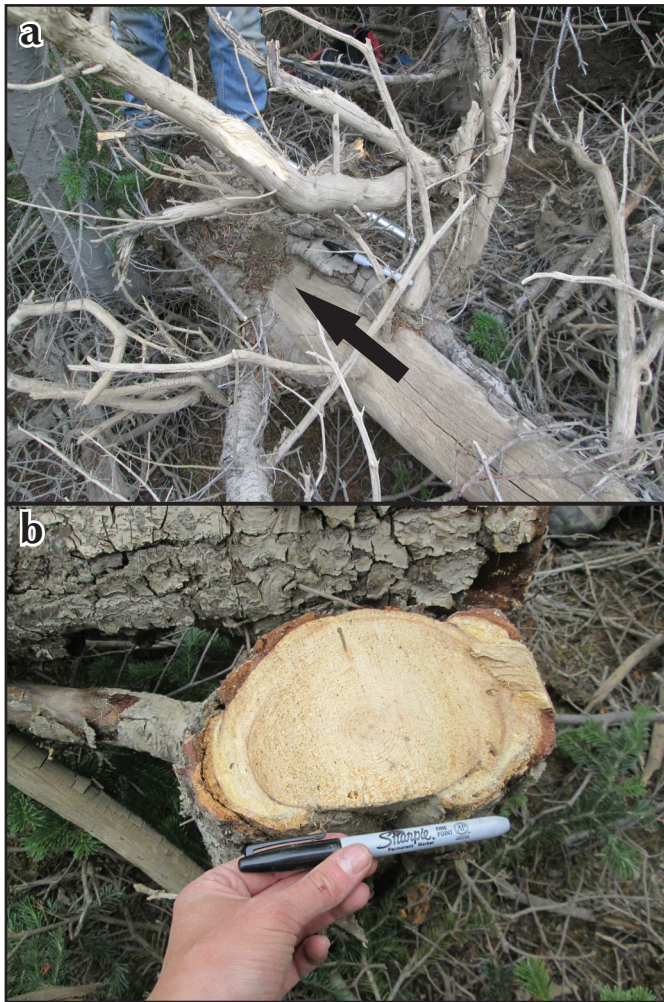


Figure 6. (a) Black arrow indicates location of cambial scarring on sample LL7b. Marker for scale. (b) Cross section of damaged tree at site LL7. Marker for scale.



Figure 7. Sample LL8 protruding from till veneer. Pencil for scale.

STUDY AREA 2 – MAIN LOBE OF LLEWELLYN GLACIER

A large gully is incised into the north lateral moraine of the main lobe of Llewellyn Glacier about 65 m above the present glacier surface (site LL9; Fig. 1). Several pieces of wood protrude from till at different elevations in this gully. Exposed along a stream flowing against the gully's southwest wall is approximately 2 m of matrix-supported, massive diamicton containing faceted striated stones up to boulder size overlying 0.5 m of weakly stratified, clast-supported diamicton (Fig. 8). Stratification in the lower unit and the sharp contact between the upper and lower units dip about 25° down the gully toward the glacier. A radiocarbon age of 910 ± 30 ^{14}C yr BP (AD 1035-1205; UCIAMS-149301) was obtained from the outer rings of a detrital subfossil branch or stem, approximately 10 cm in diameter, that protruded from the contact between the upper and lower diamicton units.



Figure 8. Red arrow points to sample LL9 protruding from a contact between coarse fluvial sediments (bottom) and till (top). Person for scale.

DISCUSSION

The north lobe of Llewellyn Glacier deposited till on top of a paleosurface developed on its east lateral moraine, about 70 m above the present ice surface, sometime between AD 260 and AD 505, based on the evidence at sites LL2 and LL10. Because the dated surface supported well-developed soil horizons and rooted trees, it is likely that the surface was exposed for at least several hundred years prior to being overridden by Llewellyn Glacier during the first half of the first millennium AD. The record at sites LL2 and LL10 is consistent with evidence that the main and south lobes advanced into mature forest between AD 300 and AD 500 (Clague et al., 2010).

Clague *et al.* (2010) presented evidence that the main lobe of Llewellyn Glacier was within 400 m of its maximum Holocene limit in the late 17th century prior to the maximum LIA advance. The radiocarbon-dated root in the paleosol at site LL5, about 4.8 km down-valley from sites LL2 and LL10, indicates that the north lobe of the glacier overtopped its lateral moraine and overrode a vegetated surface after AD 1650. The north lobe overrode a mature forest on the side of the bedrock knob about 5–10 m above the present valley floor near the LIA limit between AD 1690 and AD 1925, based on dates of the outermost rings of the sheared stump at site LL6 (Fig. 5). The stump contains 136 rings and the inner pith was dated to between AD 1445 and AD 1635, indicating that the tree was likely killed sometime in the late 16th to 18th centuries. When the glacier reached its LIA maximum position, it overrode trees and shrubs growing at the top of the bedrock knob. A date from detrital wood at site LL8 indicates that sediment was deposited on the bedrock knob sometime after AD 1665. Taking into account the findings of Clague *et al.* (2010) and evidence from sites LL5, LL6 and LL8, the north and main lobes probably reached their maximum LIA limits at the same time, after AD 1690.

The main lobe of Llewellyn Glacier was advancing as early as the 11th century. The dated stem or branch protruding from a contact between what is interpreted to be coarse fluvial sediments and overlying till in a gully on the north lateral moraine of the main lobe suggests that the glacier reached an elevation 65 m above the present ice surface after AD 1035. Crude stratification within the till dips parallel to the ground surface, indicating that at this site till was plastered onto the hillslope as the glacier thickened. Our data are consistent with an advance of the terminus of the main lobe of Llewellyn Glacier into mature forest between AD 1030 and AD 1210 (Clague *et al.*, 2010).

CONCLUSION

Data from sites along the margins of the north and main lobes of Llewellyn Glacier are in agreement with previous research findings that indicate a history of complex glacier fluctuations over the past two millennia. The north lobe thickened and advanced in the first half of the first millennium AD and probably repeatedly during the second half of the second millennium AD. Evidence found supports an advance of the main lobe of Llewellyn Glacier

after AD 1035, possibly during a period between the FMA and LIA advances during which glaciers have traditionally been thought to have been more restricted. These data add to a growing body of evidence on past rates and magnitudes of glacier fluctuations in northwest North America and provide context for hydrologic models used to predict the effect of climate variability on hydroelectric security in Yukon River Basin.

ACKNOWLEDGEMENTS

We acknowledge Yukon Energy Corporation and the Natural Sciences and Engineering Research Council (NSERC) for their financial support. We are grateful for the field assistance provided by Chad Bustin, and lab and analytical support from Bryan Mood at the University of Victoria Tree-Ring Lab. The authors would also like to thank Jeff Bond for his thoughtful review of the manuscript.

REFERENCES

- Arendt, A., Bliss, A., Bolch, T., Cogley, J.G., Gardner, A.S., Hagen, J.O., Hock, R., Huss, M., Kaser, G., Kienholz, C., Pfeffer, W.T., Moholdt, G., Paul, F., Radic, V., Andreassen, L., Bajracharya, S., Barrand, N., Beedle, M., Berthier, E., Bhambri, R., Brown, I., Burgess, E., Burgess, D., Cawkwell, F., Chinn, T., Copland, L., Davies, B., De Angelis, H., Dolgova, E., Filbert, K., Forester, R., Fountain, A., Frey, H., Giffen, B., Glasser, N., Gurney, S., Hagg, W., Hall, D., Haritashya, U.K., Hartmann, G., Helm, C., Herreid, S., Howat, I., Kapustin, G., Khromova, T., König, M., Kohler, J., Kriegel, D., Kutuzov, S., Lavrentiev, I., LeBris, R., Lund, J., Manley, W., Mayer, C., Miles, E.S., Li, X., Menounos, B., Mercer, A., Mölg, N., Mool, P., Nosenko, G., Negrete, A., Nuth, C., Pettersson, R., Racoviteanu, A., Ranzi, R., Rastner, P., Rau, F., Raup, B., Rich, J., Rott, H., Schneider, C., Seliverstov, Y., Sharp, M., Sigurðsson, O., Stokes, C., Wheate, R., Winsvold, S., Wolken, G., Wyatt, F. and Zheltyhina, N., 2014. Randolph Glacier Inventory – A dataset of global glacier outlines, version 4.0. Global Land Ice Measurements from Space, Boulder Colorado, USA, Digital Media, 56 p.
- Barrand, N.E. and Sharp, M.J., 2010. Sustained rapid shrinkage of Yukon glaciers since the 1957-1958 International Geophysical Year. *Geophysical Research Letters*, vol. 37, L07501.

- Brabets, T.P., Wang, B. and Meads, R.H., 2000. Environmental and hydrologic Overview of the Yukon River Basin, Alaska and Canada. United States Geological Survey, Water-Resources Investigations Report 99-4204, Anchorage, Alaska. 106 p.
- Bronk Ramsey, C., 2013. OxCal v. 4.2.4, <<http://c14.arch.ox.ac.uk/oxcal>> [accessed October, 2015].
- Clague, J.J., Koch, J. and Geertsema, M., 2010. Expansion of outlet glaciers of the Juneau Icefield in northwest British Columbia during the past two millennia. *The Holocene*, vol. 20, issue 3, p. 447-461.
- Comeau, L.E., Pietroniro, A. and Demuth, M.N., 2009. Glacier contribution to the North and South Saskatchewan Rivers. *Hydrological Processes*, vol. 23, issue 18, p. 2640-2653.
- Denton, G.H. and Karlén, W., 1973. Holocene climatic variations: their pattern and possible cause. *Quaternary Research*, vol. 3, issue 2, p. 155-205.
- Environment Canada, 2015. National Climate Data and Information Archive, <http://climate.weather.gc.ca/climate_normals> [accessed September, 2015].
- Guay, R., Gagnon, R. and Morin, H., 1992. A new automatic method and interactive tree-ring measurement system based on a line scan camera. *Forestry Chronicle*, vol. 68, p. 138-141.
- Hoffman, K. and Smith, D.J., 2013. Late Holocene glacial activity at Bromley Glacier, Cambria Icefield, northern British Columbia Coast Mountains, Canada. *Canadian Journal of Earth Sciences*, vol. 50, issue 6, p. 599-606.
- IPCC, 2013. Climate change 2013: The physical science basis. Contribution of Working Group I to the Fifth Assessment Report of the Intergovernmental Panel on Climate Change. Stocker, T.F., Qin, D., Plattner, G.-K., Tignor, M., Allen, S.K., Boschung, J., Nauels, A., Xia, Y., Bex, V. and Midgley, P.M. (eds.). Cambridge University Press, Cambridge, United Kingdom and New York, NY, USA, 1535 p.
- Mood, B. and Smith, D.J., 2015. Latest Pleistocene and Holocene behaviour at Franklin Glacier, Mt. Waddington area, British Columbia Coast Mountains, Canada. *The Holocene*, vol. 25, issue 5, p. 784-794.
- Northern Climate ExChange, 2014. Projected future changes in glaciers and their contribution to discharge of the Yukon River at Whitehorse. Northern Climate ExChange, Yukon Research Centre, Yukon College, Whitehorse, YT, 44 p.
- Reimer, P.J., Bard, E., Bayliss, A., Beck, J.W., Blackwell, P.G., Bronk Ramsey, C., Buck, C.E., Cheng, H., Edwards, R.L., Friedrich, M., Grootes, P.M., Guilderson, T.P., Haflidason, H., Hajdas, I., Hatté, C., Heaton, T.J., Hoffmann, D.L., Hogg, A.G., Hughen, K.A., Kaiser, K.F., Kromer, B., Manning, S.W., Niu, M., Reimer, R.W., Richards, D.A., Scott, E.M., Southon, J.R., Staff, R.A., Turney, C.S.M. and van der Plicht, J., 2013. IntCal13 and Marine13 radiocarbon age calibration curves 0-50,000 years cal BP. *Radiocarbon*, vol. 55, issue 4, p. 1869-1887.
- Reyes, A.V., Wiles, G.C., Smith, D.J., Barclay, D.J., Allen, S., Jackson, S., Larocque, S., Laxton, S., Lewis, D., Calkin, P.E. and Clague, J.J., 2006. Expansion of alpine glaciers in Pacific North America in the first millennium AD. *Geology*, vol. 34, issue 1, p. 57-60.
- Sprenke, K.F., Miller, M.M., McGee, S.R. and Adema, G.W., 1999. Canadian Landform Examples – 36: The high ice plateau of the Juneau Icefield, British Columbia: Form and dynamics. *The Canadian Geographer*, vol. 43, issue 1, p. 99-104.

